Eur. Phys. J. D **46**, 205–213 (2008)
DOI: 10.1140/epjd/e2007-00298-x

THE EUROPEAN PHYSICAL JOURNAL D

*Comment on*

# "Electron collisional excitation of argon-like Ni XI using the Breit-Pauli R-matrix method" [Eur. Phys. J. D **42**, 235–241 (2007)]

# Electron impact excitation of Ni XI

K.M. Aggarwal[a] and F.P. Keenan

Astrophysics Research Centre, School of Mathematics and Physics, Queen's University Belfast, Belfast BT7 1NN, Northern Ireland, UK

Received 25 June 2007
Published online 24 October 2007 

**Abstract.** In a recent paper, Verma et al. [Eur. Phys. J. D **42**, 235 (2007)] have reported results for energy levels, radiative rates, collision strengths, and effective collision strengths for transitions among the lowest 17 levels of the $(1s^22s^22p^6)\,3s^23p^6$, $3s^23p^53d$ and $3s3p^63d$ configurations of Ni XI. They adopted the CIV3 and $R$-matrix codes for the generation of wavefunctions and the scattering process, respectively. In this paper, through two independent calculations performed with the fully relativistic DARC (along with GRASP) and FAC codes, we demonstrate that their results are unreliable. New data are presented and their accuracy is assessed.

**PACS.** 34.80.Dp Atomic excitation and ionization by electron impact

## 1 Introduction

In a recent paper, Verma et al. [1] have reported results for energy levels, radiative rates, collision strengths ($\Omega$), and effective collision strengths ($\Upsilon$) for transitions among the lowest 17 levels of the $(1s^22s^22p^6)\,3s^23p^6$, $3s^23p^53d$ and $3s3p^63d$ configurations of Ni XI. They have adopted the CIV3 code of Hibbert [2] for the generation of wavefunctions, and the $R$-matrix code of Berrington et al. [3] for the calculations of $\Omega$ and $\Upsilon$. Additionally, they have included configuration interaction (CI) as well as one-body relativistic operators for calculating the energy levels and radiative rates ($A$-values). Similarly, they have resolved resonances in the thresholds region in order to determine values of $\Upsilon$ over a wide temperature range up to $10^7$ K. However, we have performed independent calculations adopting the GRASP (General-purpose Relativistic Atomic Structure Package) and the DARC (Dirac Atomic $R$-matrix Code) programs for the calculations of wavefunctions and the scattering process, respectively, and our results disagree with those of Verma et al. for all parameters. In order to further verify our results from GRASP and DARC, we have performed yet another calculation from the *Flexible Atomic Code* (FAC) of Gu [4], which is available from the website `http://kipac-tree.stanford.edu/fac/`. This is a fully relativistic code, providing energy levels, radiative rates and collision strengths. Thus results from FAC help in assessing the accuracy of all atomic parameters.

[a] e-mail: `K.Aggarwal@qub.ac.uk`

## 2 Energy levels

The GRASP code was originally developed as GRASP0 by Grant et al. [5] and a revised and modified version was published as GRASP1 by Dyall et al. [6], which has been further updated by Norrington (`http://www.am.qub.ac.uk/DARC/`). This is a fully relativistic code, and is based on the $jj$ coupling scheme. Further relativistic corrections arising from the Breit interaction and QED effects have also been included. Additionally, we have used the option of *extended average level* (EAL), in which a weighted (proportional to $2j+1$) trace of the Hamiltonian matrix is minimized. This produces a compromise set of orbitals describing closely lying states with moderate accuracy. Similarly, FAC is a fully relativistic code, and gives comparable results, as already shown for three Mg-like ions by Aggarwal et al. [7].

In Table 1 we compare our energies for the lowest 17 levels of the $3s^23p^6$, $3s^23p^53d$ and $3s3p^63d$ configurations of Ni XI. Included in this table are two calculations from GRASP, namely: GRASP1, which includes only the above 17 levels; GRASP2, which includes an additional 1073 levels from the $3p^43d^2$, $3s3p^53d^2$, $3s^23p^33d^3$, and $3s3p^43d^3$ configurations. Our GRASP1 calculation is the same as performed by Verma et al. [1], in particular for the determination of $\Omega$ and subsequently the values of $\Upsilon$. Our GRASP2 calculation includes the same configurations (and all levels) as considered by Verma et al. for the generation of their wavefunctions. As stated above in Section 1, we have performed another calculation from

**Table 1.** Energy levels (in Ryd) of Ni XI.

| Index | Configuration/Level | | NIST | GRASP1 | GRASP2 | FAC1 | FAC2 | FAC3 | CIV3 | MCHF |
|---|---|---|---|---|---|---|---|---|---|---|
| 1 | $3s^23p^6$ | $^1S_0$ | 0.0000 | 0.0000 | 0.0000 | 0.0000 | 0.0000 | 0.0000 | 0.0000 | 0.0000 |
| 2 | $3s^23p^53d$ | $^3P^o_0$ | 4.2766 | 4.2168 | 4.3049 | 4.2147 | 4.3020 | 4.2998 | 4.3474 | 3.9596 |
| 3 | $3s^23p^53d$ | $^3P^o_1$ | 4.3098 | 4.2520 | 4.3399 | 4.2499 | 4.3370 | 4.3349 | 4.3837 | 3.9919 |
| 4 | $3s^23p^53d$ | $^3P^o_2$ | 4.3811 | 4.3259 | 4.4135 | 4.3236 | 4.4104 | 4.4086 | 4.4572 | 4.0647 |
| 5 | $3s^23p^53d$ | $^3F^o_4$ | 4.4930 | 4.4356 | 4.5458 | 4.4311 | 4.5407 | 4.5391 | 4.6464 | 4.1845 |
| 6 | $3s^23p^53d$ | $^3F^o_3$ | 4.5285 | 4.4778 | 4.5861 | 4.4726 | 4.5805 | 4.5785 | 4.6866 | 4.2202 |
| 7 | $3s^23p^53d$ | $^3F^o_2$ | | 4.5404 | 4.6472 | 4.5353 | 4.6416 | 4.6393 | 4.7364 | 4.2777 |
| 8 | $3s^23p^53d$ | $^3D^o_3$ | 4.8043 | 4.7860 | 4.8750 | 4.7761 | 4.8663 | 4.8593 | 4.9358 | 4.4986 |
| 9 | $3s^23p^53d$ | $^1D^o_2$ | 4.8301 | 4.8258 | 4.9101 | 4.8170 | 4.9027 | 4.8953 | 4.9706 | 4.5264 |
| 10 | $3s^23p^53d$ | $^3D^o_1$ | 4.8735 | 4.8577 | 4.9445 | 4.8485 | 4.9367 | 4.9290 | 5.0260 | 4.5661 |
| 11 | $3s^23p^53d$ | $^3D^o_2$ | 4.9123 | 4.9000 | 4.9837 | 4.8912 | 4.9761 | 4.9687 | 5.0485 | 4.6045 |
| 12 | $3s^23p^53d$ | $^1F^o_3$ | 4.9485 | 4.9287 | 5.0170 | 4.9185 | 5.0079 | 5.0024 | 5.1267 | 4.6419 |
| 13 | $3s^23p^53d$ | $^1P^o_1$ | 6.1405 | 6.3833 | 6.2839 | 6.3487 | 6.2575 | 6.2574 | 6.4188 | 5.8861 |
| 14 | $3s3p^63d$ | $^3D_1$ | | 8.2831 | 7.7882 | 8.2691 | 7.7847 | 7.7562 | 7.8535 | 7.5315 |
| 15 | $3s3p^63d$ | $^3D_2$ | | 8.2945 | 7.8008 | 8.2805 | 7.7973 | 7.7687 | 7.8685 | 7.5435 |
| 16 | $3s3p^63d$ | $^3D_3$ | | 8.3132 | 7.8223 | 8.2993 | 7.8187 | 7.7904 | 7.8909 | 7.5631 |
| 17 | $3s3p^63d$ | $^1D_2$ | | 8.7836 | 8.0670 | 8.7597 | 8.0591 | 7.9965 | 9.0045 | 7.8197 |

NIST: `http://physics.nist.gov/PhysRefData/`
GRASP1: energies from the GRASP code with 17 level calculations.
GRASP2: energies from the GRASP code with 1090 level calculations.
FAC1: energies from the FAC code with 17 level calculations.
FAC2: energies from the FAC code with 1090 level calculations.
FAC3: energies from the FAC code with 6164 level calculations.
CIV3: energies of Verma et al. (2007) from the CIV3 code.
MCHF: energies of Irimia and Froese-Fischer (2003) from the MCHF code.

FAC, and included in Table 1 are our results from FAC1, which includes the same 17 levels as in GRASP1; FAC2, which includes the same 1090 levels as in GRASP2; and FAC3, which includes 6164 levels from *all* possible $n = 3$ configurations. Also given in this table are the experimentally compiled results of NIST (National Institute for Standards and Technology), which are available at their website `http://physics.nist.gov/PhysRefData/`, the unpublished results of Irimia and Froese-Fischer [8], obtained from their multi-configuration Hartree-Fock (MCHF) code and available at their website `http://www.vuse.vanderbilt.edu/~cff/mchf_collection/` and the CIV3 results of Verma et al.

With the same CI included, our results from GRASP and FAC are comparable and no significant differences are observed, as may be noted from Table 1. However, the limited calculations performed in GRASP1 and FAC1 clearly indicate the need for including additional CI, as otherwise the energy levels may be overestimated by up to 10% — see, for example, level 17 ($3s3p^63d\,^1D_2$). However, for the lowest 17 levels under consideration, additional CI as included in our FAC3 calculations is of no advantage over our corresponding results from GRASP2 and FAC2. These energy levels agree within 2% with the experimental compilations, although a comparison is only possible for the levels of the $3s^23p^6$ and $3s^23p^53d$ configurations. The MCHF results of Irimia and Froese-Fischer [8] are lower by up to 10% than the experimental values or our energy levels from GRASP2 or FAC2. On the other hand, the CIV3 results of Verma et al. [1] are larger by over 1 Ryd (up to 12%), especially for the levels of the $3s3p^63d$ configuration. However, their energy levels agree comparatively better with our GRASP1 and FAC1 calculations, which exclude all external CI. Furthermore, apart from the calculations from GRASP and FAC listed in Table 1, we have performed a series of other calculations with differing amount of CI and also including the $4\ell$ orbitals. However, the results obtained are (almost) the same as listed under columns GRASP2 and FAC2. The two-body relativistic operators excluded by Verma et al. are unlikely to make any appreciable difference, as confirmed by our extensive comparisons [7] for the energy levels of Fe XV, Co XVI and Ni XVII. The most likely reason for the inaccuracy of their energy levels is the restricted number of levels/configurations adopted from the total of 1090 levels generated from the seven configurations.

## 3 Radiative rates

In Table 2 we compare the oscillator strengths ($f$-values) for four transitions from our calculations from GRASP and FAC with those of Irimia and Froese-Fischer [8] from MCHF and Verma et al. [1] from CIV3. The calculations from GRASP1 and FAC1 are included here to demonstrate, once again, the importance of additional CI as included in the GRASP2, FAC2 and FAC3 results. Except for the 1–13 ($3s^23p^6\,^1S_0$ – $3s^23p^53d\,^1P^o_1$) transition, the $f$-values from GRASP1 and FAC1 are *higher* by over an order of magnitude, whereas more extensive CI included in FAC3 is of no additional advantage in comparison to the results from GRASP2 and FAC2. Our (converged) $f$-values from both the GRASP and FAC codes also agree with

**Table 2.** Comparison of oscillator strengths ($f$-values) for transitions in Ni XI. $a \pm b \equiv a \times 10^{\pm b}$.

| $i$ | $j$ | Transition | GRASP1 | GRASP2 | FAC1 | FAC2 | FAC3 | MCHF | CIV3 |
|---|---|---|---|---|---|---|---|---|---|
| 1 | 13 | $3s^23p^6\,{}^1\mathrm{S}_0 - 3s^23p^5 3d\,{}^1\mathrm{P}^\mathrm{o}_1$ | 3.453–0 | 2.624–0 | 3.442–0 | 2.601–0 | 2.657–0 | 2.528–0 | 2.575–0 |
| 9 | 17 | $3s^23p^5 3d\,{}^1\mathrm{D}^\mathrm{o}_2 - 3s3p^6 3d\,{}^1\mathrm{D}_2$ | 1.008–1 | 1.319–2 | 1.010–1 | 1.356–2 | 1.084–2 | 2.555–2 | 1.586–1 |
| 12 | 17 | $3s^23p^5 3d\,{}^1\mathrm{F}^\mathrm{o}_3 - 3s3p^6 3d\,{}^1\mathrm{D}_2$ | 1.180–1 | 1.626–2 | 1.171–1 | 1.659–2 | 1.411–2 | 2.290–2 | 1.816–1 |
| 13 | 17 | $3s^23p^5 3d\,{}^1\mathrm{P}^\mathrm{o}_1 - 3s3p^6 3d\,{}^1\mathrm{D}_2$ | 1.190–1 | 7.533–3 | 1.208–1 | 7.971–3 | 4.797–3 | 8.143–3 | 1.136–1 |

GRASP1: 17 level calculations from the GRASP code.
GRASP2: 1090 level calculations from the GRASP code.
FAC1: 17 level calculations from the FAC code.
FAC2: 1090 level calculations from the FAC code.
FAC3: 6164 level calculations from the FAC code.
MCHF: calculations of Irimia and Froese-Fischer (2003) from the MCHF code.
CIV3: calculations of Verma et al. (2007) from the CIV3 code.

**Table 3.** Collision strengths for transitions in Ni XI at energies above thresholds (in Ryd). $a \pm b \equiv a \times 10^{\pm b}$.

| Transition | | Energy (Ryd) | | | | | | | | | | |
|---|---|---|---|---|---|---|---|---|---|---|---|---|
| $i$ | $j$ | 10 | 20 | 40 | 60 | 80 | 100 | 120 | 140 | 160 | 180 | 200 |
| 1 | 2 | 9.477−3 | 6.132−3 | 2.836−3 | 1.589−3 | 1.014−3 | 7.009−4 | 5.154−4 | 3.934−4 | 3.113−4 | 2.527−4 | 2.082−4 |
| 1 | 3 | 2.923−2 | 1.940−2 | 9.936−3 | 6.392−3 | 4.815−3 | 4.001−3 | 3.557−3 | 3.296−3 | 3.149−3 | 3.070−3 | 3.036−3 |
| 1 | 4 | 4.607−2 | 2.980−2 | 1.381−2 | 7.737−3 | 4.933−3 | 3.410−3 | 2.507−3 | 1.914−3 | 1.514−3 | 1.229−3 | 1.013−3 |
| 1 | 5 | 3.570−2 | 2.144−2 | 9.727−3 | 5.453−3 | 3.484−3 | 2.407−3 | 1.767−3 | 1.348−3 | 1.063−3 | 8.595−4 | 7.090−4 |
| 1 | 6 | 2.883−2 | 1.867−2 | 1.062−2 | 7.893−3 | 6.742−3 | 6.171−3 | 5.872−3 | 5.703−3 | 5.608−3 | 5.557−3 | 5.559−3 |
| 1 | 7 | 1.891−2 | 1.134−2 | 5.144−3 | 2.886−3 | 1.847−3 | 1.279−3 | 9.422−4 | 7.210−4 | 5.708−4 | 4.633−4 | 3.837−4 |
| 1 | 8 | 2.764−2 | 2.556−2 | 2.631−2 | 2.821−2 | 2.989−2 | 3.126−2 | 3.236−2 | 3.328−2 | 3.405−2 | 3.472−2 | 3.548−2 |
| 1 | 9 | 1.138−2 | 6.667−3 | 2.926−3 | 1.649−3 | 1.084−3 | 7.805−4 | 6.010−4 | 4.828−4 | 4.011−4 | 3.426−4 | 2.973−4 |
| 1 | 10 | 2.094−2 | 2.142−2 | 2.365−2 | 2.583−2 | 2.772−2 | 2.941−2 | 3.097−2 | 3.243−2 | 3.383−2 | 3.521−2 | 3.661−2 |
| 1 | 11 | 1.129−2 | 6.593−3 | 2.795−3 | 1.521−3 | 9.713−4 | 6.840−4 | 5.176−4 | 4.097−4 | 3.364−4 | 2.847−4 | 2.448−4 |
| 1 | 12 | 4.028−2 | 4.024−2 | 4.452−2 | 4.866−2 | 5.190−2 | 5.442−2 | 5.642−2 | 5.807−2 | 5.943−2 | 6.061−2 | 6.194−2 |
| 1 | 13 | 3.677+0 | 4.532+0 | 5.707+0 | 6.486+0 | 7.073+0 | 7.553+0 | 7.973+0 | 8.353+0 | 8.707+0 | 9.046+0 | 9.382+0 |
| 1 | 14 | 1.115−2 | 7.155−3 | 3.550−3 | 2.057−3 | 1.326−3 | 9.176−4 | 6.708−4 | 5.100−4 | 4.008−4 | 3.219−4 | 2.643−4 |
| 1 | 15 | 1.884−2 | 1.227−2 | 6.257−3 | 3.799−3 | 2.593−3 | 1.922−3 | 1.517−3 | 1.255−3 | 1.077−3 | 9.497−4 | 8.584−4 |
| 1 | 16 | 2.593−2 | 1.669−2 | 8.258−3 | 4.789−3 | 3.086−3 | 2.137−3 | 1.562−3 | 1.188−3 | 9.333−4 | 7.495−4 | 6.154−4 |
| 1 | 17 | 2.301−1 | 2.731−1 | 3.157−1 | 3.388−1 | 3.523−1 | 3.612−1 | 3.677−1 | 3.729−1 | 3.774−1 | 3.814−1 | 3.856−1 |

those of Irimia and Froese-Fischer, although their result is higher by a factor of two for the 9–17 ($3s^23p^5 3d\,{}^1\mathrm{D}^\mathrm{o}_2$ – $3s3p^6 3d\,{}^1\mathrm{D}_2$) transition. On the other hand, the CIV3 results of Verma et al. only agree with the other calculations for the 1–13 ($3s^23p^6\,{}^1\mathrm{S}_0$ – $3s^23p^5 3d\,{}^1\mathrm{P}^\mathrm{o}_1$) transition, and are *overestimated* for other transitions by over an order of magnitude. However, their $f$-values for three transitions are comparable with those obtained from our GRASP1 (or FAC1) calculation, due to the restricted number of levels/configurations adopted by them, as suggested above in Section 1, and can be noted from their Table 2. Therefore, it may be concluded without any ambiguity that the reported $f$-values by Verma et al. are overestimated, because of the inclusion of limited CI.

## 4 Collision strengths

For the computations of collision strengths $\Omega$, we have employed the *Dirac Atomic R-matrix Code* (DARC) of Norrington and Grant [9], as implemented by Ait-Tahar et al. [10]. This program includes the relativistic effects in a systematic way, in both the target description and the scattering model. It is based on the $jj$ coupling scheme, and uses the Dirac-Coulomb Hamiltonian in the $R$-matrix approach. The $R$-matrix radius has been adopted to be 2.97 au, and 19 continuum orbitals have been included for each channel angular momentum for the expansion of the wavefunction. This allows us to compute $\Omega$ up to an energy of 220 Ryd. The maximum number of channels for a partial wave is 81, and the corresponding size of the Hamiltonian matrix is 1544. In order to obtain convergence of $\Omega$ for all transitions and at all energies, we have included all partial waves with angular momentum $J \leq 39.5$, although a larger number would have been preferable for the convergence of allowed transitions, especially at higher energies. However, to account for the inclusion of higher neglected partial waves, we have included a top-up, based on the Coulomb-Bethe approximation for allowed transitions and geometric series for others.

Our second calculation for $\Omega$ has been performed with the FAC code, which like DARC is a fully relativistic code, and is based on the well-known and widely used *distorted-wave* (DW) method. However, this code only provides the *background* values of $\Omega$, and hence resonances in thresholds region are not resolved from these calculations. Nevertheless, independent calculations from FAC will be greatly helpful in assessing the accuracy of values of $\Omega$.

The computed values of $\Omega$ for transitions from the ground state $3s^23p^6\,{}^1\mathrm{S}_0$ to higher excited levels are listed in Table 3, at energies above thresholds in the range $10 \leq E \leq 200$ Ryd. In this energy range $\Omega$ varies

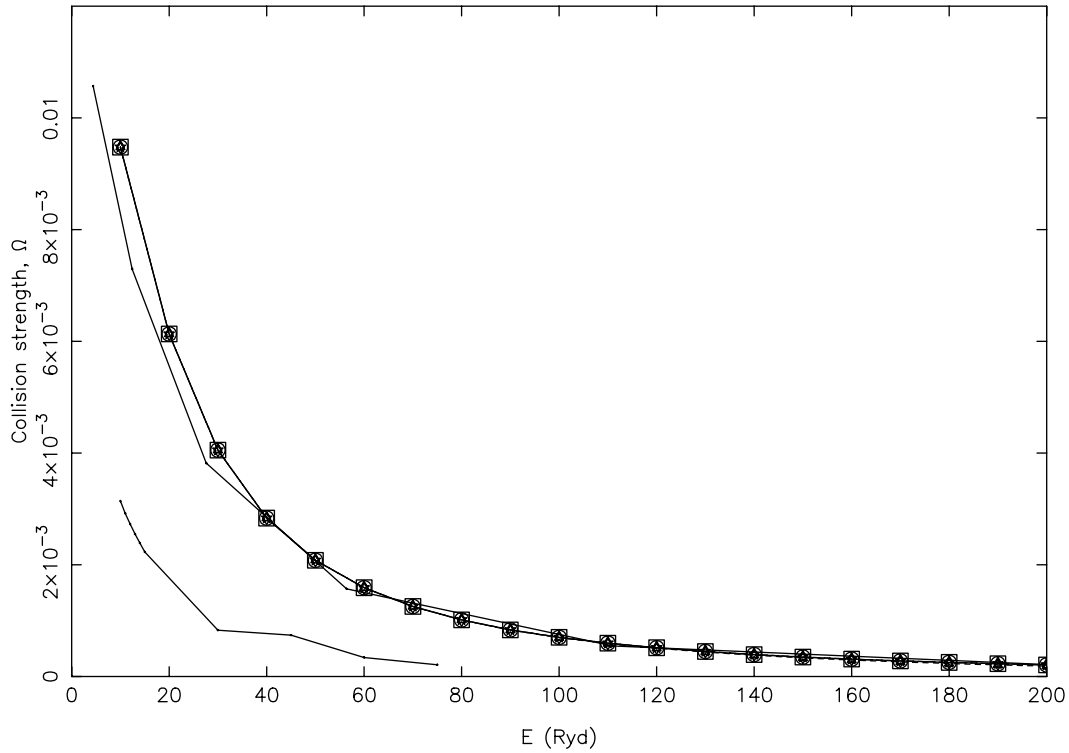


**Fig. 1.** Comparison of total collision strength ($\Omega$) for the 1–2 ($3s^2 3p^6\ ^1\mathrm{S}_0$ – $3s^2 3p^5 3d\ ^3\mathrm{P}^\mathrm{o}_0$) transition of Ni XI at energies above thresholds (in Ryd). Lower continuous curve — results of Verma et al. [1], upper continuous curve — present results from FAC, broken curves are our present results from DARC, triangles: $J \leq 9.5$, diamonds: $J \leq 19.5$, squares: $J \leq 29.5$, circles: $J \leq 39.5$, and stars are the converged values with top-up.

smoothly, and hence the corresponding value at any desired energy within this range can easily be interpolated. In Figures 1–3 we compare our results of $\Omega$ with those of Verma et al. [1] for the 1–2 ($3s^2 3p^6\ ^1\mathrm{S}_0$ – $3s^2 3p^5 3d\ ^3\mathrm{P}^\mathrm{o}_0$), 1–13 ($3s^2 3p^6\ ^1\mathrm{S}_0$ – $3s^2 3p^5 3d\ ^1\mathrm{P}^\mathrm{o}_1$) and 1–17 ($3s^2 3p^6\ ^1\mathrm{S}_0$ – $3s 3p^6 3d\ ^1\mathrm{D}_2$) transitions, respectively. Also included in this figure are our corresponding results obtained from the FAC code. Additionally, our results from DARC are shown here with increasing number of partial waves, which clearly demonstrates the importance of higher partial waves, neglected by Verma et al. The 1–2 transition is forbidden, and values of $\Omega$ have *converged* within $J \leq 9.5$ at all energies. Similarly, there is complete agreement between our results from DARC and FAC, but the corresponding $\Omega$ values of Verma et al. are clearly underestimated by over a factor of two in the entire common energy range. Since they have included the contribution from all partial waves with $L \leq 9$, their $\Omega$ values should have been comparable to ours.

The 1–13 transition is *allowed* for which the $\Omega$ values have been compared in Figure 2 at energies below 200 Ryd. Allowed transitions converge slowly, and the contribution of higher partial waves becomes increasingly important with increasing energy, as may be noted from Figure 2. At energies above 50 Ryd, even a large range of $J \leq 39.5$ is not sufficient to obtain converged results for $\Omega$, and hence a top-up becomes necessary. Therefore, it is clear from Figure 2 that the $\Omega$ values of Verma et al. are highly *underestimated* at all energies. Additionally, at an energy of 10 Ryd, the contribution of $J \leq 9.5$ is nearly sufficient to obtain the converged results, yet the $\Omega$ values of Verma et al. are lower by a factor of four. Furthermore, $\Omega$ values for electric dipole transitions increase with increasing energy [11], as is also evident from our calculations from DARC and FAC, whereas the corresponding results of Verma et al. decrease with increasing energy for all transitions, as may be noted from their Table 5. Even for some forbidden transitions, such as 1–17 for which $\Omega$ values are compared in Figure 3, a large range of partial waves is required to obtain the converged results for collision strengths. For this transition the $\Omega$ values of Verma et al. are underestimated by an order of magnitude, whereas there is no discrepancy between the corresponding results obtained from DARC and FAC. Therefore, based on the comparisons shown for three transitions in Figures 1–3 and similar comparisons performed for other transitions (but not shown here), it will be reasonable to conclude that the $\Omega$ values reported by Verma et al. are not reliable for any transition and at any energy.

Our results for $\Omega$ listed in Table 3 are assessed to be accurate to better than 10% for all transitions and at all energies. This assessment is based on the comparison made between the calculations performed with the DARC and FAC codes. However, since these calculations have been performed with the limited 17 level model ion, this assessment is not rigorous. Therefore, a larger calculation

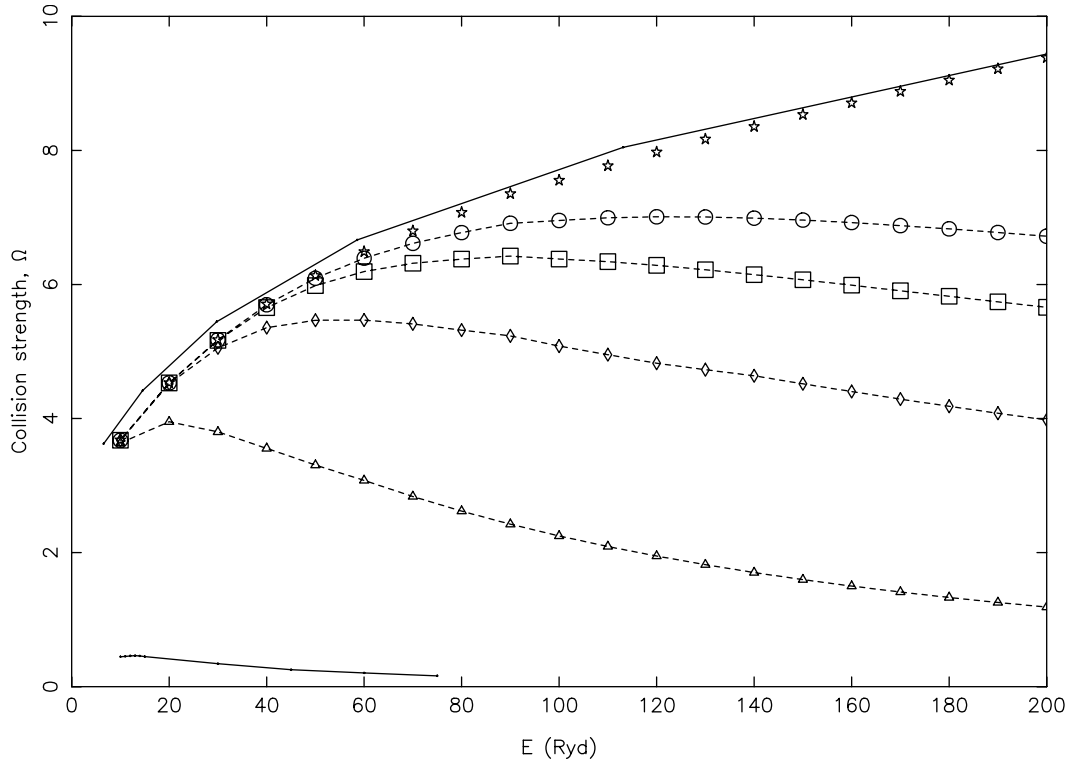


**Fig. 2.** Comparison of total collision strength ($\Omega$) for the 1–13 ($3s^2 3p^6\ ^1\mathrm{S}_0 - 3s^2 3p^5 3d\ ^1\mathrm{P}^{\mathrm{o}}_1$) transition of Ni XI at energies above thresholds (in Ryd). Lower continuous curve — results of Verma et al. [1], upper continuous curve — present results from FAC, broken curves are our present results from DARC, triangles: $J \leq 9.5$, diamonds: $J \leq 19.5$, squares: $J \leq 29.5$, circles: $J \leq 39.5$, and stars are the converged values with top-up.

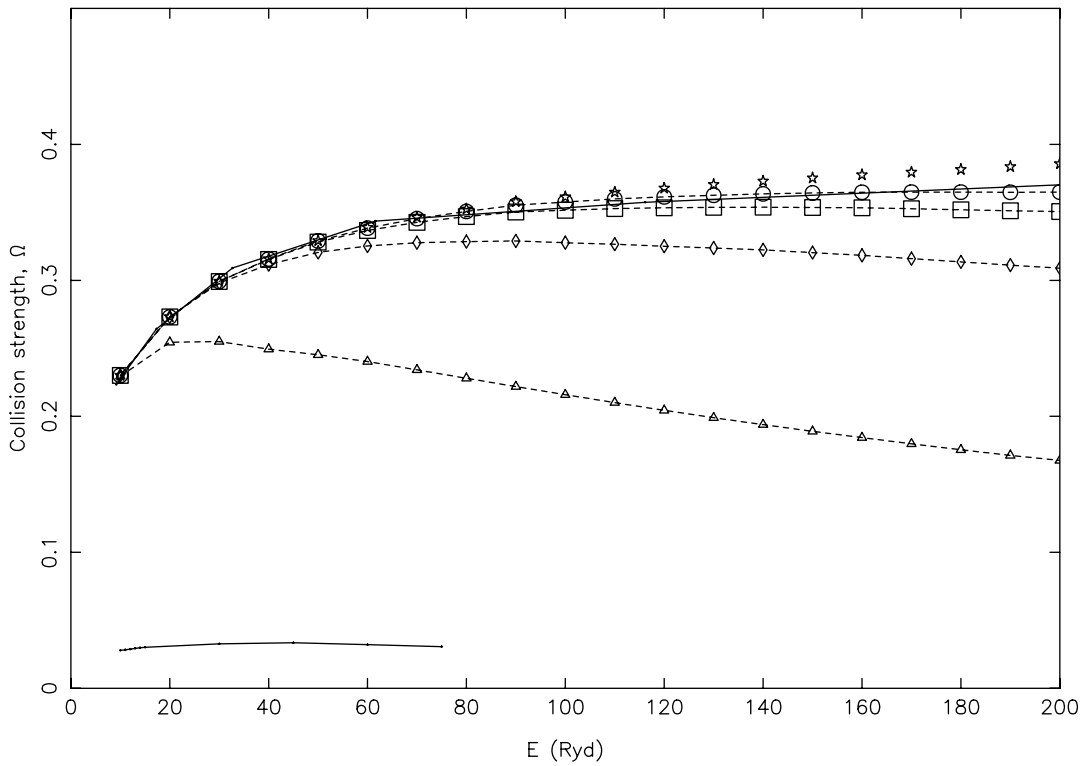


**Fig. 3.** Comparison of total collision strength ($\Omega$) for the 1–17 ($3s^2 3p^6\ ^1\mathrm{S}_0 - 3s 3p^6 3d\ ^1\mathrm{D}_2$) transition of Ni XI at energies above thresholds (in Ryd). Lower continuous curve — results of Verma et al. [1], upper continuous curve — present results from FAC, broken curves are our present results from DARC, triangles: $J \leq 9.5$, diamonds: $J \leq 19.5$, squares: $J \leq 29.5$, circles: $J \leq 39.5$, and stars are the converged values with top-up.

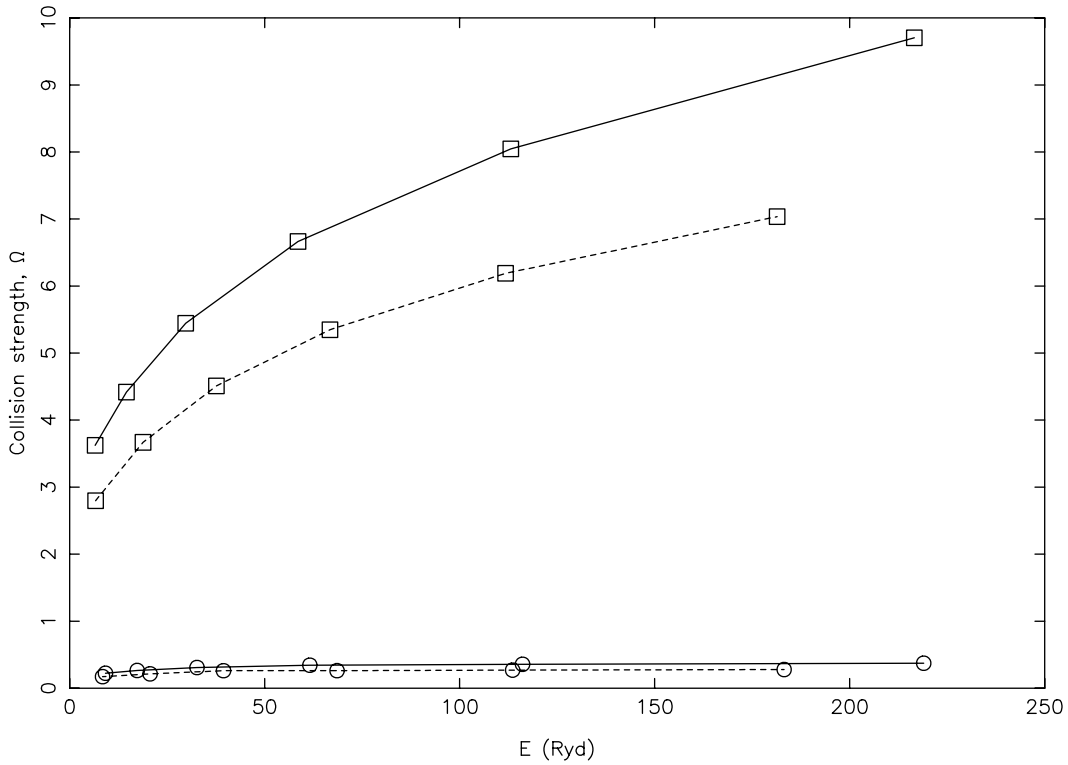


**Fig. 4.** Collision strength ($\Omega$) at energies above thresholds (in Ryd). Continuous curves: FAC1, broken curves: FAC2, squares are for the 1–13 ($3s^2 3p^6\ ^1\mathrm{S}_0$ – $3s^2 3p^5 3d\ ^1\mathrm{P}^\mathrm{o}_1$) and circles are for the 1–17 ($3s^2 3p^6\ ^1\mathrm{S}_0$ – $3s 3p^6 3d\ ^1\mathrm{D}_2$) transition of Ni XI.

needs to be performed as for the energy levels and $A$-values. A large calculation with 1090 levels (corresponding to GRASP2 configurations) is not feasible with the DARC code, but is possible with the FAC code. Therefore, we have performed another calculation with the FAC code with all the 1090 levels belonging to the seven configurations of the GRASP2 and FAC2, listed above in Section 2. A comparison between the FAC1 and FAC2 calculations of $\Omega$ for the transitions of Table 3 shows an agreement within 10% for all transitions except four, namely 1–13, 1–14, 1–15 and 1–17. For these four transitions, the discrepancy is up to 25% as shown in Figure 4 for the 1–13 and 1–17 transitions, which have comparatively larger values of $\Omega$. The 1–13 transition is allowed and the other three are forbidden. For the 1–13 ($3s^2 3p^6\ ^1\mathrm{S}_0$ – $3s^2 3p^5 3d\ ^1\mathrm{P}^\mathrm{o}_1$) transition, the $f$-value in the FAC2 (and GRASP2) calculations is lower by ∼25% than in the FAC1 (or GRASP1) calculation (see Tab. 2), and this is directly reflected in the lower values of $\Omega$ obtained in FAC2. These differences for some transitions are therefore due to the improvement in wavefunctions achieved with the inclusion of larger CI. To conclude, we may state that the values of $\Omega$ listed in Table 3 are accurate to better than 25%.

## 5 Effective collision strengths

Effective collision strengths ($\Upsilon$) are obtained after integrating the $\Omega$ data over a Maxwellian distribution of electron velocities as follows:

$$\Upsilon(T_e) = \int_0^\infty \Omega(E) \exp(-E_j/kT_e) d(E_j/kT_e), \quad (1)$$

where $k$ is Boltzmann constant, $T_e$ is electron temperature in K, and $E_j$ is the electron energy with respect to the final (excited) state. Once the value of $\Upsilon$ is known the corresponding results for excitation and de-excitation rates can be easily obtained, as shown in equations (2–3) of Aggarwal et al. [12].

Since the threshold region is dominated by numerous resonances, $\Omega$ must be computed in a fine mesh of energy. Therefore, we have computed values of $\Omega$ at over 2700 energies in the threshold region with $\Delta E \leq 0.002$ Ryd. This fine energy mesh ensures to a large extent that neither a majority of resonances are missed, nor do the exceptionally high resonances have unreasonably large width. In Figures 5 and 6 we show resonances for only two transitions, namely 1–2 ($3s^2 3p^6\ ^1\mathrm{S}_0$ – $3s^2 3p^5 3d\ ^3\mathrm{P}^\mathrm{o}_0$) and 1–13 ($3s^2 3p^6\ ^1\mathrm{S}_0$ – $3s^2 3p^5 3d\ ^1\mathrm{P}^\mathrm{o}_1$), because similar results from the calculations of Verma et al. [1] are available for comparison.

For the 1–13 transition, resonances are not important as shown in Figure 6, because it is an allowed transition. However, our background values of $\Omega$ are stable in the entire threshold energy region, and rise with increasing energy as already shown in Figure 2 and listed in Table 3. The corresponding results of Verma et al. [1] are underestimated as discussed above, because of the limited range of partial waves included. This has a very significant effect

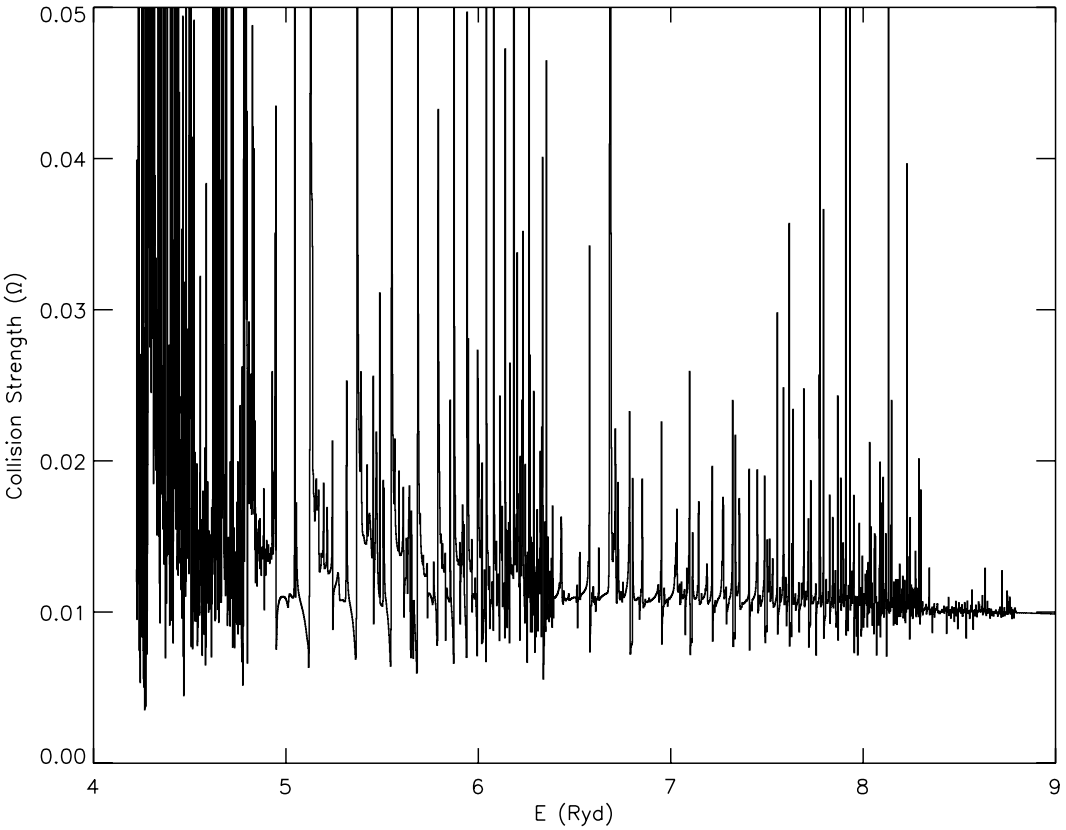


**Fig. 5.** Collision strength ($\Omega$) in thresholds region for the 1–2 ($3s^2 3p^6\ ^1\mathrm{S}_0$ – $3s^2 3p^5 3d\ ^3\mathrm{P}^{\mathrm{o}}_0$) transition of Ni XI.

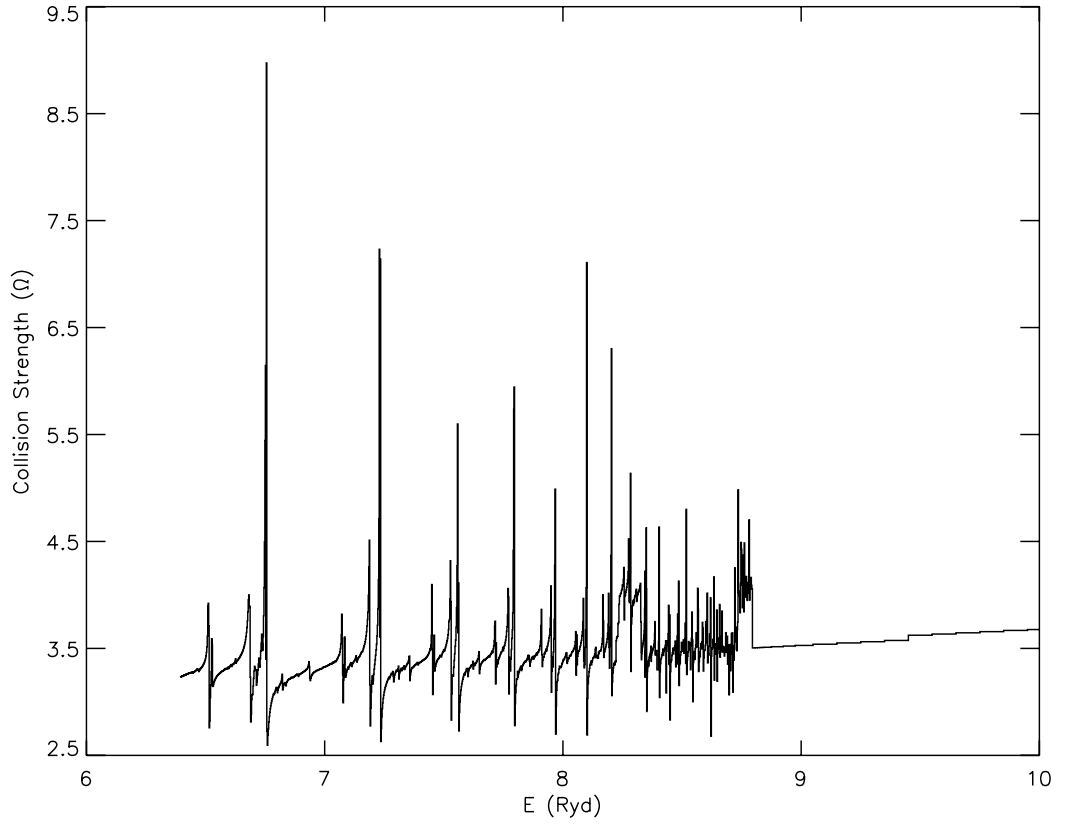


**Fig. 6.** Collision strength ($\Omega$) in thresholds region for the 1–13 ($3s^2 3p^6\ ^1\mathrm{S}_0$ – $3s^2 3p^5 3d\ ^1\mathrm{P}^{\mathrm{o}}_1$) transition of Ni XI.

**Table 4.** Effective collision strengths for transitions in Ni XI. $a \pm b \equiv a \times 10^{\pm b}$.

| Transition | | Temperature ($10^5$ K) | | | | | | | | | | |
|---|---|---|---|---|---|---|---|---|---|---|---|---|
| $i$ | $j$ | 1.0 | 2.0 | 4.0 | 6.0 | 8.0 | 10.0 | 20.0 | 40.0 | 60.0 | 80.0 | 100.0 |
| 1 | 2 | 3.502−2 | 2.575−2 | 1.923−2 | 1.634−2 | 1.457−2 | 1.332−2 | 9.888−3 | 6.962−3 | 5.489−3 | 4.566−3 | 3.923−3 |
| 1 | 3 | 1.249−1 | 9.247−2 | 6.812−2 | 5.696−2 | 5.017−2 | 4.546−2 | 3.310−2 | 2.332−2 | 1.862−2 | 1.573−2 | 1.371−2 |
| 1 | 4 | 2.027−1 | 1.516−1 | 1.105−1 | 9.181−2 | 8.051−2 | 7.268−2 | 5.220−2 | 3.594−2 | 2.808−2 | 2.325−2 | 1.991−2 |
| 1 | 5 | 1.374−1 | 1.081−1 | 8.259−2 | 6.969−2 | 6.147−2 | 5.558−2 | 3.974−2 | 2.705−2 | 2.101−2 | 1.732−2 | 1.479−2 |
| 1 | 6 | 1.934−1 | 1.388−1 | 9.666−2 | 7.760−2 | 6.630−2 | 5.865−2 | 3.998−2 | 2.708−2 | 2.152−2 | 1.825−2 | 1.603−2 |
| 1 | 7 | 1.735−1 | 1.147−1 | 7.517−2 | 5.868−2 | 4.923−2 | 4.296−2 | 2.799−2 | 1.784−2 | 1.348−2 | 1.094−2 | 9.248−3 |
| 1 | 8 | 1.264−1 | 1.110−1 | 8.804−2 | 7.423−2 | 6.532−2 | 5.914−2 | 4.457−2 | 3.641−2 | 3.384−2 | 3.246−2 | 3.133−2 |
| 1 | 9 | 9.752−2 | 8.484−2 | 6.644−2 | 5.434−2 | 4.615−2 | 4.027−2 | 2.537−2 | 1.532−2 | 1.123−2 | 8.941−3 | 7.462−3 |
| 1 | 10 | 2.961−2 | 2.881−2 | 2.684−2 | 2.561−2 | 2.483−2 | 2.432−2 | 2.343−2 | 2.385−2 | 2.460−2 | 2.505−2 | 2.510−2 |
| 1 | 11 | 6.438−2 | 6.708−2 | 5.607−2 | 4.676−2 | 4.012−2 | 3.525−2 | 2.260−2 | 1.382−2 | 1.017−2 | 8.118−3 | 6.783−3 |
| 1 | 12 | 1.598−1 | 1.504−1 | 1.223−1 | 1.041−1 | 9.225−2 | 8.411−2 | 6.540−2 | 5.592−2 | 5.347−2 | 5.222−2 | 5.100−2 |
| 1 | 13 | 3.372+0 | 3.454+0 | 3.603+0 | 3.732+0 | 3.845+0 | 3.948+0 | 4.383+0 | 5.045+0 | 5.503+0 | 5.776+0 | 5.894+0 |
| 1 | 14 | 1.440−2 | 1.296−2 | 1.165−2 | 1.085−2 | 1.025−2 | 9.747−3 | 7.994−3 | 6.053−3 | 4.934−3 | 4.187−3 | 3.646−3 |
| 1 | 15 | 2.409−2 | 2.176−2 | 1.965−2 | 1.837−2 | 1.738−2 | 1.655−2 | 1.365−2 | 1.042−2 | 8.567−3 | 7.324−3 | 6.421−3 |
| 1 | 16 | 3.280−2 | 2.972−2 | 2.689−2 | 2.513−2 | 2.377−2 | 2.262−2 | 1.858−2 | 1.407−2 | 1.147−2 | 9.731−3 | 8.475−3 |
| 1 | 17 | 2.254−1 | 2.299−1 | 2.368−1 | 2.425−1 | 2.475−1 | 2.520−1 | 2.695−1 | 2.919−1 | 3.047−1 | 3.098−1 | 3.090−1 |

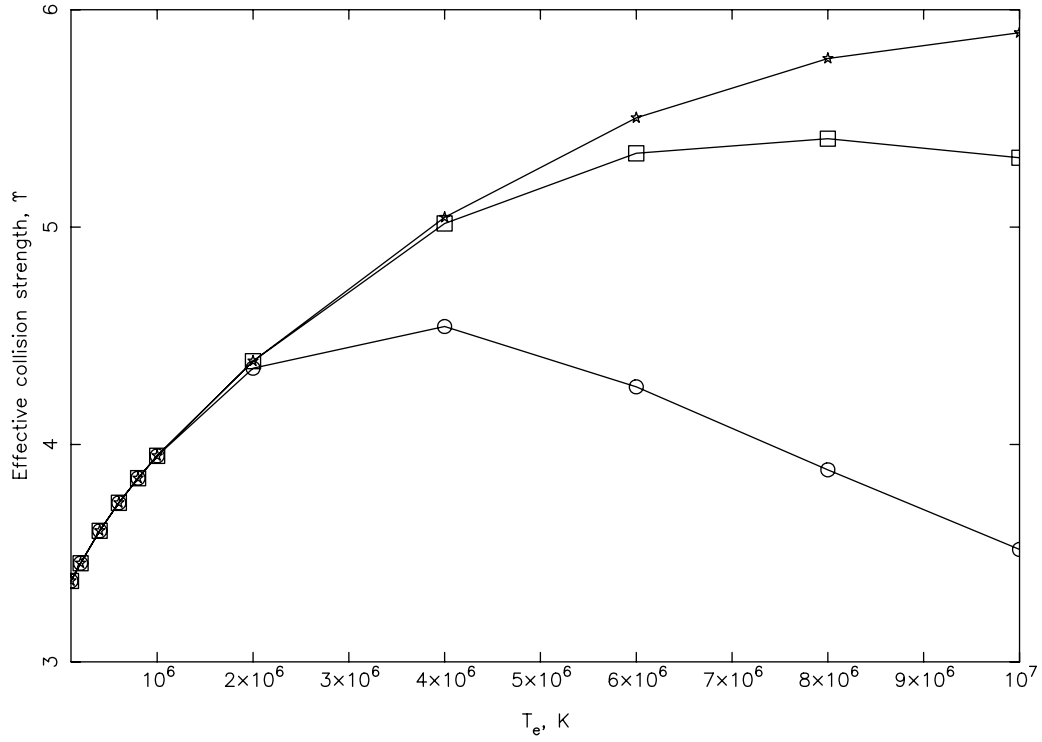


**Fig. 7.** Effective collision strength ($\Upsilon$) for the 1–13 ($3s^2 3p^6\ ^1\mathrm{S}_0$ – $3s^2 3p^5 3d\ ^1\mathrm{P}^\mathrm{o}_1$) transition of Ni XI. Lower curve (circles) is obtained with $E \leq 75$ Ryd, middle curve (squares) with $E \leq 150$ Ryd, and upper curve (stars) give final converged results.

on the values of $\Upsilon$, which we will discuss below. Similarly, even for the 1–2 (and other) forbidden transition(s), their $\Omega$ values are not only underestimated, but also decrease to almost zero at some energies as shown in their Figure 2, whereas we do not observe any such behaviour. This is again due to the limited range of partial waves adopted by these authors.

In Table 4 we list our values of $\Upsilon$ for all 16 transitions from the ground state to higher excited levels of Ni XI over a wide temperature range of $10^5$ to $10^7$ K, suitable for applications in astrophysical, fusion and laser-produced plasmas. The only other similar results available in the literature for comparison are those of Verma et al. [1], which are in complete disagreement with ours, because their $\Omega$ values are in error. Additionally, further errors are inhibited into their values of $\Upsilon$, because of the limited range of energy ($E \leq 75$ Ryd) adopted by them. This energy range is *not* sufficient for the convergence of the integral in equation (1) up to the temperature of $10^7$ K. To demonstrate the deficiency of their calculations we show our values of $\Upsilon$ for only one transition, namely 1–13 ($3s^2 3p^6\ ^1\mathrm{S}_0$ – $3s^2 3p^5 3d\ ^1\mathrm{P}^\mathrm{o}_1$) in Figure 7. The lowest

curve (circles) correspond to the calculations of $\Upsilon$ performed using values of $\Omega$ at $E \leq 75$ Ryd, the middle curve (squares) corresponds to $E \leq 150$ Ryd, and the top curve (stars) gives the converged results, listed in Table 4. It is clear from this figure that $E \leq 75$ Ryd provides values of $\Upsilon$, which are underestimated by up to a factor of two, depending on the temperature. The corresponding results obtained with $E \leq 150$ Ryd are also underestimated, but only by up to 10%. Increasing the energy range beyond 220 Ryd makes an insignificant difference to the $\Upsilon$ values listed in Table 4.

## 6 Conclusions

In this paper, we have presented results for energy levels, radiative rates, collision strengths, and effective collision strengths for transitions from the ground state to higher excited levels of Ni XI. The corresponding available results of Verma et al. [1] are assessed to be unreliable for all parameters. Their data for energy levels and radiative rates are overestimated because of the limited CI included. In addition, their reported values of $\Omega$ and $\Upsilon$ are underestimated by over an order of magnitude for some of the transitions, because of the inclusion of a limited range of partial waves and scattering energy, respectively.

The results reported in this paper have been determined with as much accuracy as possible, as demonstrated by a variety of comparisons. However, they do have scope for further improvement. This is mainly because the electron-ion model considered here is small and is only for demonstration purposes. To improve the accuracy of all parameters a much larger model needs to be considered, as discussed in Sections 2, 3 and 4 regarding the determination of energy levels, radiative rates, and collision strengths, respectively. A larger model will also improve the accuracy of the desired values of $\Upsilon$, because resonances arising from the higher excited levels may enhance the results for transitions among the lower levels. However, until such calculations become available the presently reported results can be applied with confidence to the analysis of Ni XI transitions observed from high temperature plasmas [13].

This work has been financed by the Engineering and Physical Sciences and Particle Physics and Astronomy Research Councils of the United Kingdom, and FPK is grateful to AWE Aldermaston for the award of a William Penney Fellowship.

## References

1. N. Verma, A.K.S. Jha, M. Mohan, Eur. Phys. J. D **42**, 235 (2007)
2. A. Hibbert, Comput. Phys. Commun. **9**, 141 (1975)
3. K.A. Berrington, W.B. Eissner, P.H. Norrington, Comput. Phys. Commun. **92**, 290 (1995)
4. M.F. Gu, Astrophys. J. **582**, 1241 (2003)
5. I.P. Grant, B.J. McKenzie, P.H. Norrington, D.F. Mayers, N.C. Pyper, Comput. Phys. Commun. **21**, 207 (1980)
6. K.G. Dyall, I.P. Grant, C.T. Johnson, F.A. Parpia, E.P. Plummer, Comput. Phys. Commun. **55**, 424 (1989)
7. K.M. Aggarwal, V. Tayal, G.P. Gupta, F.P. Keenan, At. Data Nucl. Data Tables **93**, 615 (2007)
8. A. Irimia, C. Froese-Fischer, available at `http://www.vuse.vanderbilt.edu/~cff/mchf_collection/` (2003)
9. P.H. Norrington, I.P. Grant, in preparation
10. S. Ait-Tahar, I.P. Grant, P.H. Norrington, Phys. Rev. A **54**, 3984 (1996)
11. A. Burgess, J.A. Tully, Astron. Astrophys. **254**, 436 (1992)
12. K.M. Aggarwal, F.P. Keenan, Pramana - J. Phys. **69**, 209 (2007)
13. M. Mattioli, K.B. Fournier, I. Coffey, M. Finkenthal, C. Jupén, M. Valisa, Contributors to the EFDA-JET Work Programme, J. Phys. B **37**, 13 (2004)